Targeting Chromatin Regulators Inhibits Leukemogenic Gene Expression in *NPM1* Mutant Leukemia

- Supplemental Figures, Tables, and Methods -

Michael W.M. Kühn[1,2], Evelyn Song[1], Zhaohui Feng[1], Amit Sinha[1], Chun-Wei Chen[1], Aniruddha J. Deshpande[1], Monica Cusan[1], Noushin Farnoud[1], Annalisa Mupo[5], Carolyn Grove[6,7], Richard Koche[1], James E. Bradner[3], Elisa de Stanchina[4], George S. Vassiliou[5], Takayuki Hoshii[1], and Scott A. Armstrong[1,8]

(1) Cancer Biology and Genetics Program, Memorial Sloan Kettering Cancer Center, NY, NY, USA
(2) Department of Medicine III, University Medical Center, Johannes Gutenberg-University, Mainz, Germany
(3) Department of Medical Oncology, Dana-Farber Cancer Institute, Harvard Medical School, Boston, MA, USA
(4) Antitumor Assessment Facility, Memorial Sloan Kettering Cancer Center, NY, NY, USA.
(5) Wellcome Trust Sanger Institute, Hinxton, Cambridge, UK
(6) Department of Haematology, PathWest/Sir Charles Gairdner Hospital, Nedlands, WA, Australia
(7) School of Pathology and Laboratory Medicine, University of Western Australia, Crawley, WA, Australia
(8) Department of Pediatric Oncology, Dana-Farber Cancer Institute, and Division of Hematology/Oncology, Boston Children's Hospital, Harvard Medical School, Boston, MA, USA

Corresponding Author:
Scott A. Armstrong, MD, PhD, Department of Pediatric Oncology, Dana-Farber Cancer Institute, Harvard Medical School, 450 Brookline Avenue, Boston, MA 02215, U.S.A., Phone: +1-617-632-3644, Fax: +1-617-632-4367, e-mail: scott_armstrong@dfci.harvard.edu

Supplemental Fig. 1

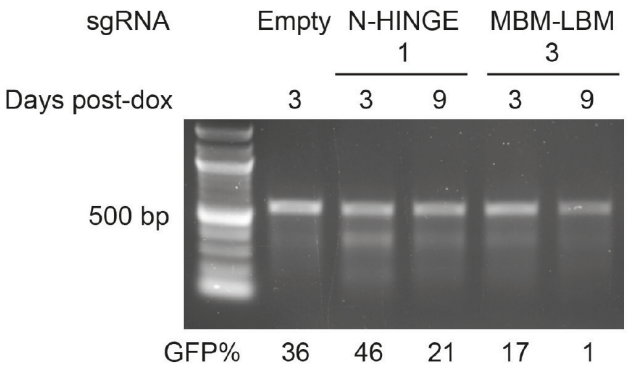

Supplemental Fig.2

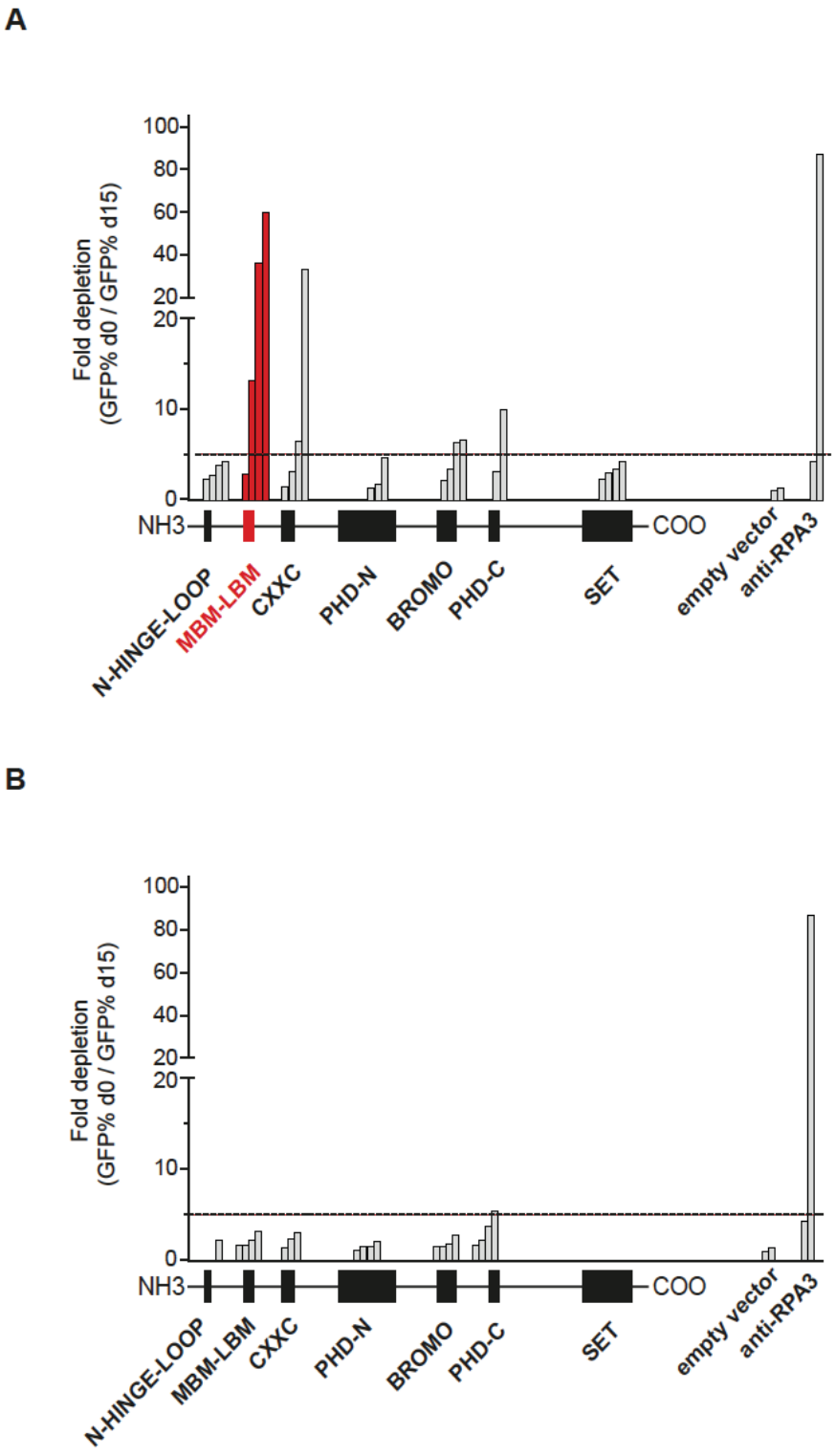

Supplemental Fig.3

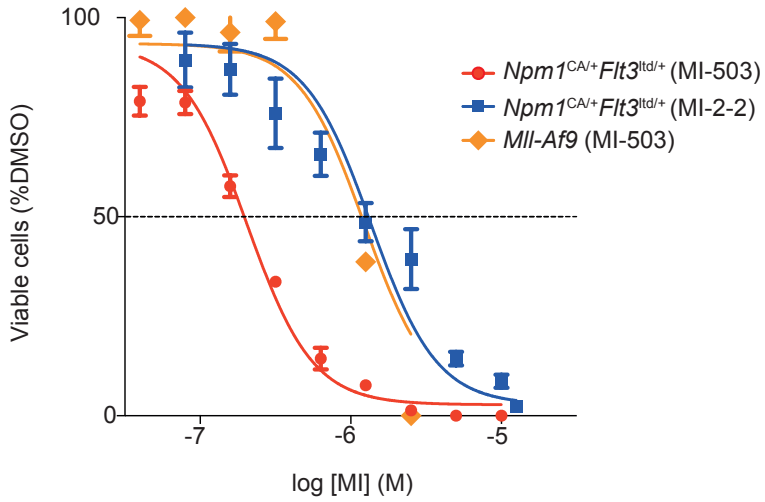

Supplemental Fig.4

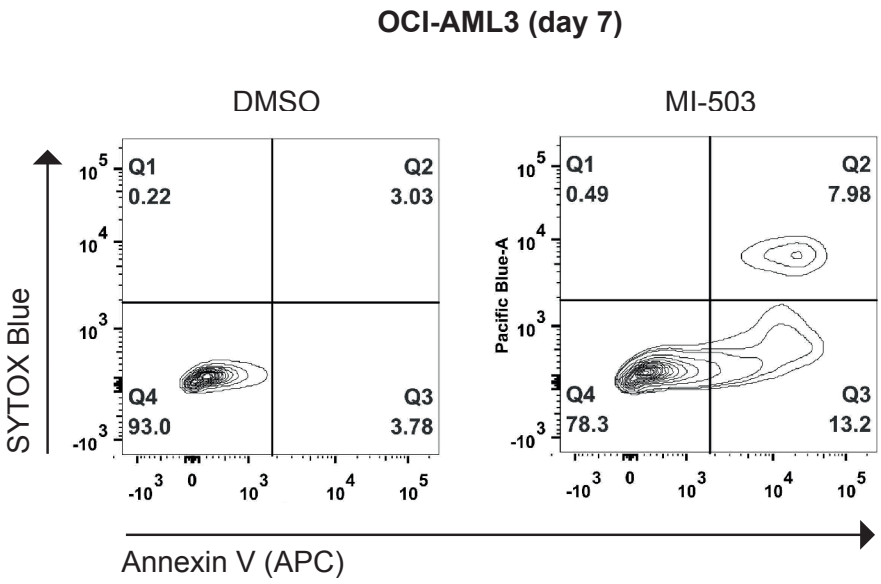

Supplemental Fig.5

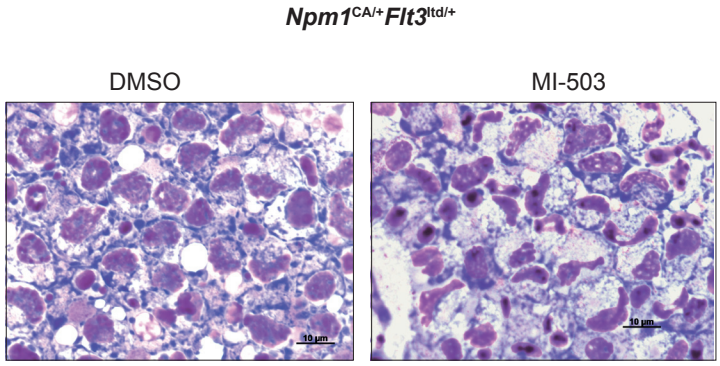

Supplemental Fig.6

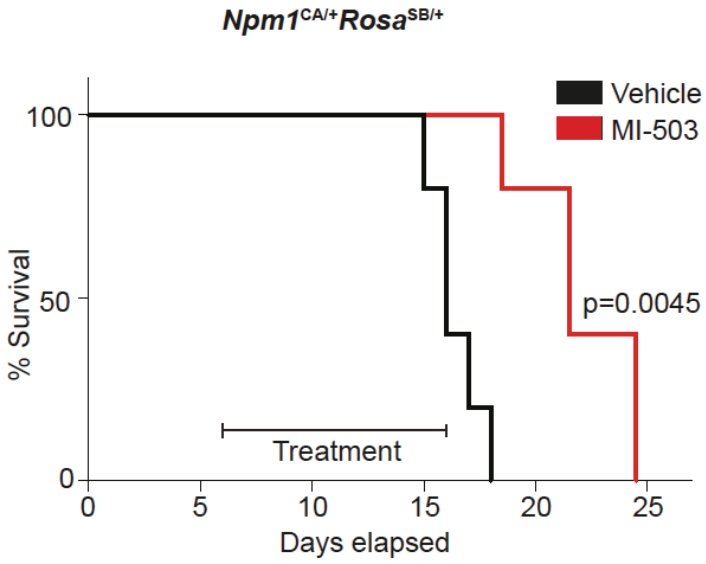

Supplemental Fig.7

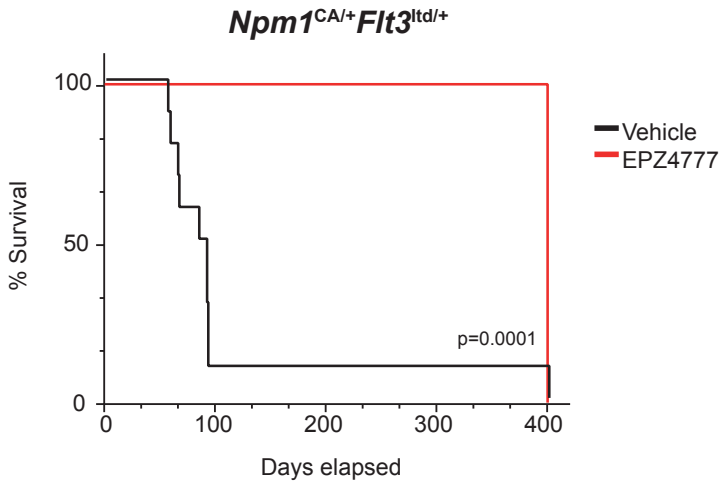

Supplemental Fig.8

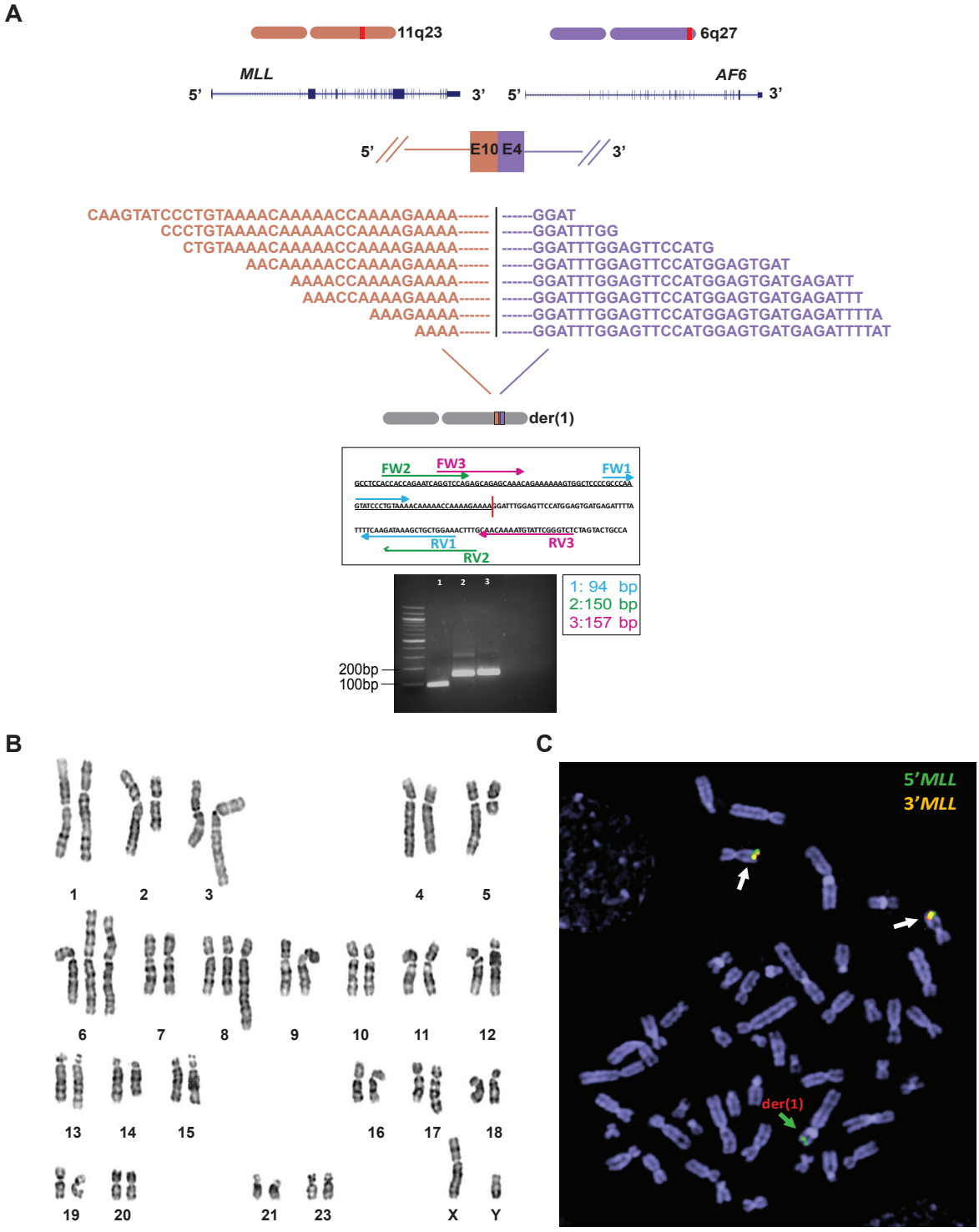

Supplemental Fig.9

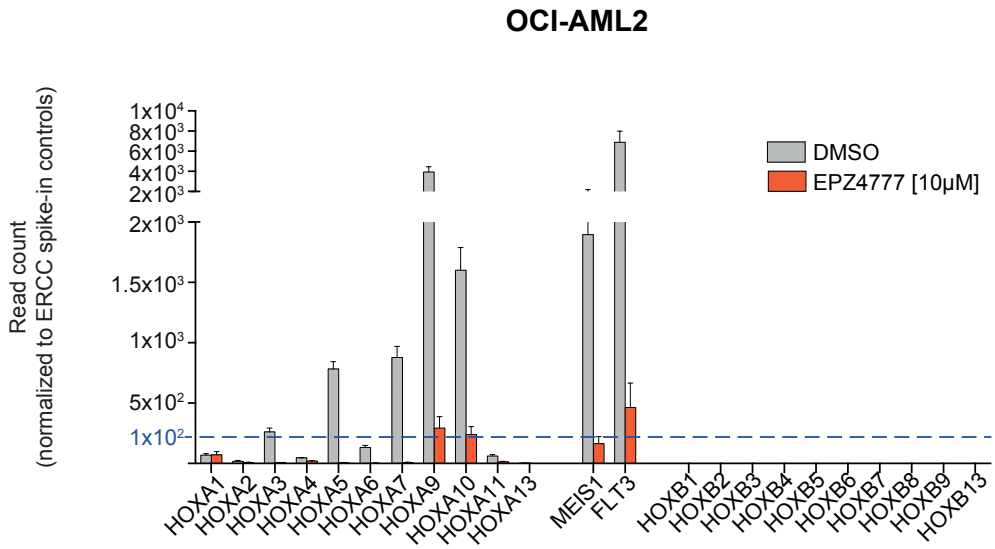

Supplemental Fig.10

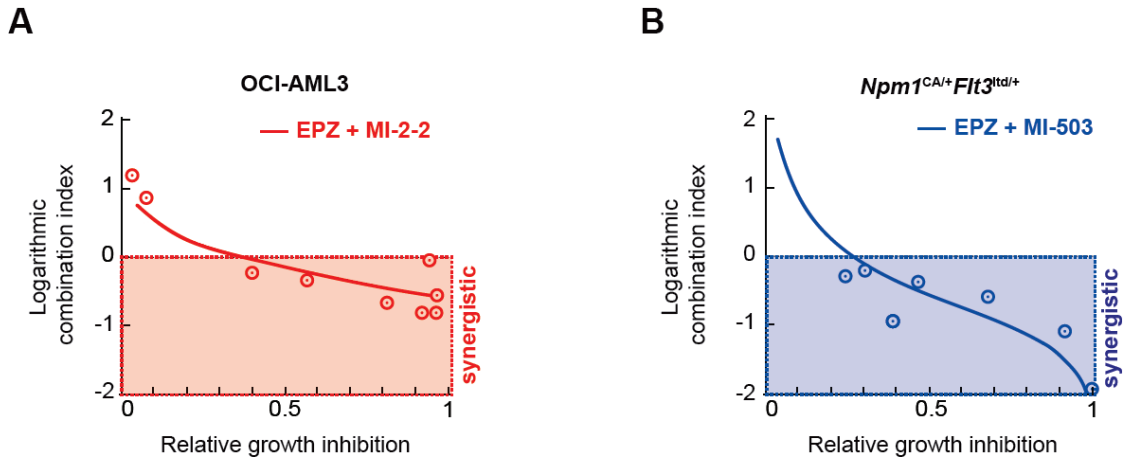

Supplemental Fig.11

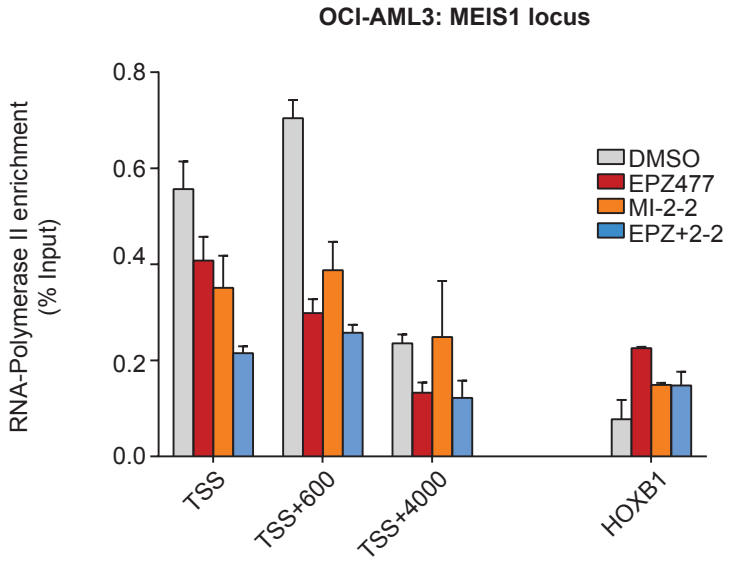

Supplemental Fig.12

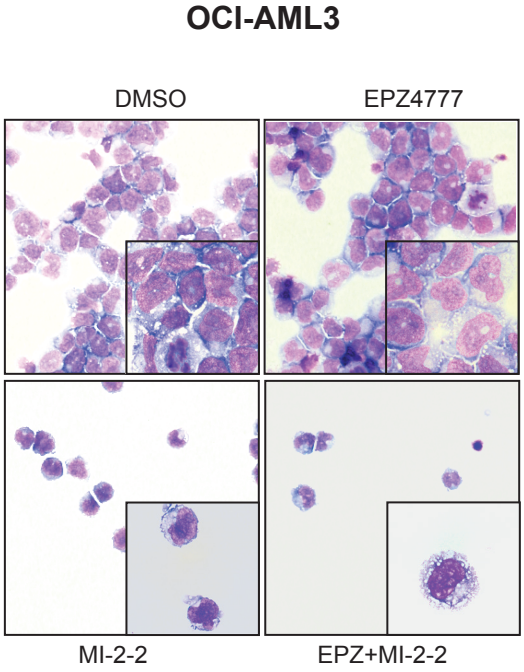

Supplemental Fig. 13

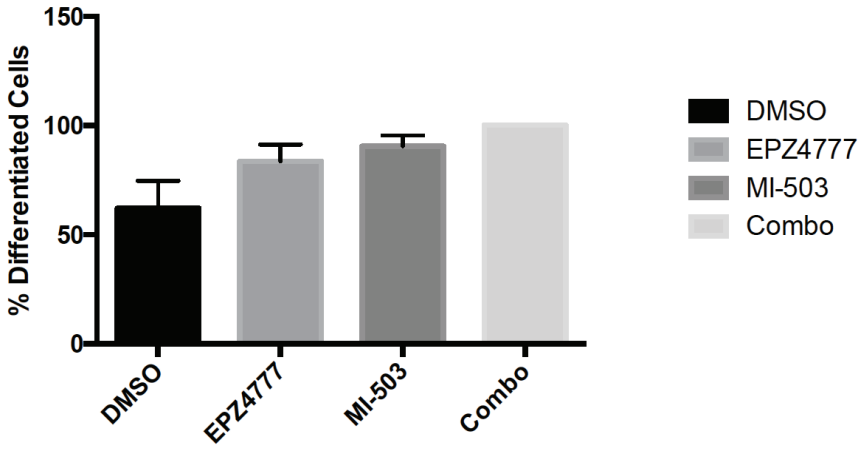

Supplemental Fig.14

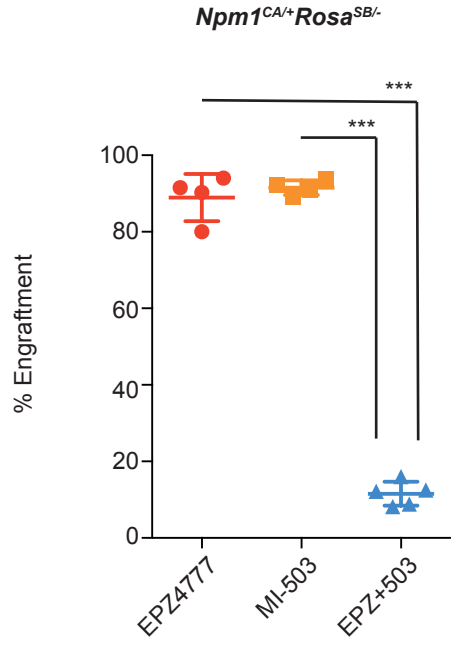

SUPPLEMENTAL FIGURE LEGENDS

Supplemental Fig.1:

SURVEYOR assay assessing indel mutations of sgRNAs that target the N-HINGE-LOOP and the MBM-LBM locus. Analysis was performed at day 3 and at day 9 post Caspase 9 induction (doxycyline (dox) treatment start). Empty vector (empty) sgRNA serves as a negative control. The GFP^+ percentages of each sample are labeled under the gel image.

Supplemental Fig.2:

(**A** and **B**) Summary of negative selection experiments with sgRNAs targeting exons encoding specific MLL1 and MLL2 protein domains in a second independent OCI-AML3-Cas9 clone (OCI-AML3-Cas9-C8). Negative selection is plotted as the fold depletion of GFP^+ cells (d0 GFP% divided by d15 GFP%) during 18 days in culture. Each bar represents an independent sgRNA. The location of each sgRNA relative to the MLL1 or MLL2 protein is indicated along the *x* axis. The dashed line indicates a fivefold change. The data shown are the mean value of two independent replicates. Empty vector and anti-RPA3 sgRNA represent negative and positive controls.

Supplemental Fig.3:

Dose response curves from cell viability assays of murine *Npm1*$^{CA/+}$*Flt3*$^{ITD/+}$ after 7 days of MI-2-2 or MI-503 treatment and compared to *Mll-Af9* leukemia cells treated for 7 days with MI-503.

Supplemental Fig.4:

Apoptosis in OCI-AML3 cells treated for 7 days with MI-503 or DMSO as assessed by Annexin V / SYTOX blue staining. To calculate percentages of apoptotic cells, fractions of early apoptotic (Annexin V-pos./ SYTOX Blue-neg.) and late apoptotic (Annexin V-pos. / SYTOX Blue-pos.) cells were combined.

Supplemental Fig.5:

Cytospins from cultured murine *Npm1*$^{CA/+}$*Flt3*$^{ITD/+}$ comparing cells treated for 7 days with MI-503 versus DMSO.

Supplemental Fig.6:

Kaplan-Meier survival estimates from mice transplanted with secondary *Npm1*$^{CA/+}$*Rosa*$^{SB/+}$ leukemia cells (n=5 mice/group) and treated *in vivo* for ten consecutive days with either MI-503 (50mg/kg bid IP) or vehicle control (25% DMSO, 25% PEG400, and 50% H_2O). MI-503 resulted in a significant increase in survival for the treated mice compared to vehicle control (increase of median survival 31%, p=0.0045).

Supplemental Fig.7:

Kaplan-Meier estimates of mice transplanted with secondary *Npm1*$^{CA/+}$*Flt3*$^{ITD/+}$ leukemia cells (n=10 mice/group) that had been pretreated with either 10 days of EPZ4777 [10µM] or vehicle prior to transplantation. EPZ4777 treatment caused significantly reduced leukemia initiation potential of pretreated cells and resulted in a profound survival advantage of the pretreated cells (p=0.0001). At day 400 all mice from the control group were electively sacrificied.

Supplemental Fig.8:

(**A**) Schematic of RNA sequencing detecting an *MLL-AF6* fusion transcript (**upper panel**) in the *DNMT3A* mutated AML cell line OCI-AML2. The fusion of exon 10 of the *MLL* and exon 4 of the *AF6* gene was confirmed using three breakpoint spanning primer sets (**lower panel**). (**B**) Conventional cytogenetics confirmed the published complex karyotype for this cell line with two normal *MLL* loci at chromosome 11q23 and the known derivative chromosome 1. (**C**) Fluorescence in-situ hybridization (FISH) analysis confirmed two normal 5' and 3' *MLL* signals at both chromosomes 11q23 but a 5'*MLL* split signal mapping to the derivative chromosome 1.

(fw=forward primer; rv=reverse primer).

Supplemental Fig.9:

RNA sequencing of the OCI-AML2 cells reveals a *HOX* gene expression pattern as it is typically found in *MLL*-rearranged leukemias with predominant *HOXA* and *MEIS1* expression but lack of *HOXB* cluster expression. The *HOXA* cluster and *MEIS1* expression is profoundly down regulated upon 7 days of treatment with EPZ4777 (10µM).

Supplemental Fig.10:

Isobolograms showing drug synergism for (**A**) MI-2-2 and EPZ4777 in the OCI-AML3 cells and (**B**) MI-503 and EPZ4777 in the murine *Npm1*$^{CA/+}$*Flt3*$^{ITD/+}$ cells. Synergism was calculated using the Chou-Talalay algorithm via CompuSyn software. Logarithmic Combination indices below 0 prove synergism for the respective concentrations as indicated.

Supplemental Fig.11:

ChIP-PCR assessing RNA-Polymerase II enrichment after vehicle, single drug (MI-503 or EPZ4777) or combination treatment at the *MEIS1* locus (at the transcriptional start site (TSS), 600 bp downstream of the TSS, and 4000 bp downstream of the TSS).

Supplemental Fig.12:

Cytologic analysis of human OCI-AML3 cells treated with DMSO, MI-2-2 (12µM), EPZ4777 (10µM), or combination therapy (MI-2-2 + EPZ4777), consistent with more profound differentiation within the combination group.

Supplemental Fig. 13:

Number of morphologically differentiated cells of two primary AML samples (ID1 and ID3) that had been treated in a human co-culture assay for 10 days with DMSO, EPZ4777, MI-503, or EPZ4777 and MI-503 (combo). For the analysis, cells were morphologically dichotomized in either Blast-like (including cells from all morphological stages between blasts and metamyelocyte-like cells) and differentiated (containing mainly macrophages and neutrophils).

Supplemental Fig.14:

Engraftment of *Npm1*$^{CA/+}$*Rosa*$^{SB/+}$ leukemia cells in the peripheral blood of tertiary recipient animals 22 days after transplantations. The plot compares animals injected with pretreated cells (DMSO, EPZ4777 [10µM], MI-503 [2.5µM], and combinatorial EPZ4777 plus MI-503 treatment) at the timepoint when first death occurred within the treatment group.

Supplemental Table 1: *MLL1* single guide RNAs (sgRNA)

sgRNA Name	Target + PAM Sequence	Quality Score
N-HINGE-LOOP-1	CGCCCCGCGGCAACGCGTCCCGG	91
N-HINGE-LOOP-2	GGGCCGCCACCGCCGACCGGGGG	87
N-HINGE-LOOP-3	CGAAGACGAGGCGGACGACGAGG	78
N-HINGE-LOOP-4	TGACGAAGACGAAGACGAGGCGG	54
MBM-LBM-1	TGCAGCGCCGCGTCGAAGCCCGG	93
MBM-LBM-2	GCACCAACCTGCGCCGGTTCCGG	93
MBM-LBM-3	CTGCAGGTCTCGGCCGCCATCGG	84
MBM-LBM-4	GGTGGGCCCGGGCTTCGACGCGG	84
CXXC-1	GACGTCGATCGAGGCGGTGTGGG	99
CXXC-2	TATATTGCGACCACCAAACTTGG	82
CXXC-3	TGCTTAGATAAGCCCAAGTTTGG	72
CXXC-4	GTACAAACACCACAGTCCTCAGG	70
PHD-N-1	AGAGGAGAACGAGCGCCCTCTGG	84
PHD-N-2	TGCAAATTCTGTCACGTTTGTGG	81
PHD-N-3	ACTCAGGGTGATAGCTGTTTCGG	77
PHDC-1	TGTGAGACAGCAACCCACGGTGG	82
PHDC-2	ACACATGAAGTGATAGTTGCTGG	74
BROM-1	CCATTTGCTACGCTACCGGCAGG	96
BROM-2	GTCTCGGGATTTAAGTCTGGAGG	84
BROM-3	TGGTGGATCAGGTCCTTCGGGGG	84
BROM-4	CAGCAGCCTTTAGATCTAGAAGG	78
SET-1	GATGGAGCGGATGACGTTGCCGG	89
SET-2	AAAAGACCCCGGCCATGGATGGG	81
SET-3	GGAAAAGTATTACGACAGCAAGG	80
SET-4	GAGATGGTGATTGAGTATGCCGG	77

N-HINGE-LOOP= N-terminal hinge loop of the menin binding domain of MLL1 that spans a large distance on menin without many specific interactions. MBM-LBM=N-terminal fragment of MLL1 containing the menin-binding and the LEDGF-binding motif (as defined by Huang et al[1]), CXXC= CXXC domain; PHD-N=N-terminal PHD-finger domains; PHD-C=C-terminal PHD-finger domain; BROM=Bromodomain; SET=Set domain.

All sgRNAs targeting the MBM-LBM coding exon are targeting the alpha2 helix in MLL1 as defined by Huang et al.[1] in MLL1 that interacts with menin and LEDGF. Numbering (1-4) of the individual sgRNAs targeting the sequence of the same domain, were ordered and numbered based on measured GFP fold depletion and do not reflect a positional order.

Supplemental Table 2: *MLL2* single guide RNAs

sgRNA Name	Target + PAM Sequence	Quality Score
N-HINGE-LOOP-1	CCCCGTTGCCCCGTCCGCCGCGG	89
N-HINGE-LOOP-2	CAACGGGGCCGAAAGAGTGCGGG	83
MBM-LBM-1	ACGGCCCTGCTCCGTTTGCTGGG	87
MBM-LBM-2	CGTTTGCTGGGGCTCCGCCGGGG	84
MBM-LBM-3	GAGCCCCAGCAAACGGAGCAGGG	76
MBM-LBM-4	GGCCGTGTCCTCCCCGGGCTCGG	60
CXXC-1	AAGATGCGCATGGCTCGATGTGG	91
CXXC-2	TCGGGGCTGCCTACGTGTGCAGG	90
CXXC-4	GGTGTTAGGGCCCCCAAACTTGG	82
PHD-N-1	CAGCTCGTGGAGTCCTTTGCTGG	78
PHD-N-2	AGCACCAGGTGTCGTGATGCTGG	90
PHD-N-3	CCACGCGCAAACGGCGCCACTGG	97
PHD-N-4	TGCATACCACCCGGCCTGTCTGG	89
PHDC-1	AGTGCGCACAGTGCGATCACTGG	94
PHDC-2	TCATAGCAGCGTGTACAGATCGG	87
PHDC-3	CTGGTCGGCGGAAGTCTTCGAGG	90
PHDC-4	CTGAAGCCTGGCGCCACGGTGGG	84
BROM-1	AGCTGTGAGTCAGCGCTTCGAGG	90
BROM-2	ACTCACAGCTTGCAGGCCGCAGG	76
BROM-3	GATGGGAAGCAACTGCACCCAGG	71
BROM-4	CAGCAGTGGGCCCACCACCTTGG	62
SET-1	TAAGCGCAACATCGACGCGGGGG	98
SET-2	CGGGTGCTATATGTTCCGCATGG	93
SET-3	GGCGGCATTGCCATGCATCGTGG	93

N-HINGE-LOOP= N-terminal hinge loop of the menin binding motif of MLL2 that spans a large distance on menin without many specific interactions. MBM-LBM=N-terminal fragment of MLL1 containing the menin-binding and the LEDGF-binding motif (as defined by Huang et al.[1]), CXXC= CXXC domain; PHD-N=N-terminal PHD-finger domains; PHD-C=C-terminal PHD-finger domain; BROM=Bromodomain; SET=Set domain.

Supplemental Table 3: Synergy analysis of OCI-AML3 cells (day 7)

EPZ4777		MI-2-2		EPZ+MI-2-2		
Dose [µM]	**Effect**	**Dose [µM]**	**Effect**	**Dose [µM]**	**Effect**	**Log(CI)***
10.0	**0.82252**	12	**0.76**	22	**0.94**	**-0.0321**
5.0	**0.7787**	6	**0.68**	11	**0.97**	**-0.5495**
2.5	**0.74626**	3	**0.49**	5.5	**0.96**	**-0.8043**
1.25	**0.69816**	1.5	**0.24**	2.75	**0.92**	**-0.8069**
0.625	**0.61478**	0.75	**0.11**	1.375	**0.81**	**-0.6644**
0.3125	**0.46254**	0.375	**0.06**	0.6875	**0.57**	**-0.3210**
0.15625	**0.30157**	0.1875	**0.05**	0.34375	**0.40**	**-0.2047**

Log(CI)=Logarithmic combination index; logarithmic values below 0 indicate synergism;
Effect=Relative growth inhibition

Supplemental Table 4: Synergy analysis of *Npm1*$^{CA/+}$*Flt3*$^{ITD/+}$ leukemias (day 11)

EPZ4777		MI-503		EPZ+503		
Dose [µM]	**Effect**	**Dose [µM]**	**Effect**	**Dose [µM]**	**Effect**	**Log(CI)***
10.0	**0.49**	2.5	**0.86**	12.5	**1.00**	**n.a.**
5.0	**0.48**	1.25	**0.66**	6.25	**0.99**	**-1.8579**
2.5	**0.35**	0.625	**0.52**	3.125	**0.91**	**-1.0409**
1.25	**0.30**	0.3125	**0.33**	1.5625	**0.68**	**-0.5509**
0.625	**0.27**	0.15625	**0.20**	0.78125	**0.47**	**-0.3555**
0.3125	**0.23**	0.07813	**0.16**	0.39063	**0.31**	**-0.2000**
0.15625	**0.15**	0.03906	**0.13**	0.19531	**0.25**	**-0.2726**

Log(CI)=Logarithmic combination index; logarithmic values below 0 indicate synergism;
Effect=Relative growth inhibition

Supplemental Table 5: Primary AML samples

ID	AML type	Cytogenetics	Mutated Genes
1	**De novo**	**Normal**	***NPM1***
2	**De novo**	**Normal**	***NPM1***
3	**De novo**	**Normal**	***NPM1, FLT3*-ITD**
4	**De novo**	**Normal**	***NPM1, FLT3*-ITD, *DNMT3A***
5*	**De novo**	**Normal**	***NPM1, FLT3-ITD***

*Cells were not maintainable in culture

SUPPLEMENTAL METHODS

Cell Culture and Cell Lines

The AML cell lines OCI-AML3, MOLM13, HL60 were cultured under standard conditions using RPMI and OCI-AML2 in alpha-MEM all supplemented with 10% fetal bovine serum (FBS) and 1% Penicillin/Streptomycin (PS). SET2 cells were maintained in RPMI with 20% FBS and 1% PS; 293T and Hs27cells both in DMEM with 10% FBS and 1% PS. Cell line authentication testing (ATCC) verified identity and purity for all human AML cell lines used in this study. Murine leukemia cells were cultured in DMEM supplemented with 15% FBS, 1% PS, and cytokines (SCF 100ng/µl, IL-3 20ng/µl, and IL-6 20ng/µl).

CRISPR-Cas9 Screening

Plasmid construction and sgRNA design: The pCW-Cas9 expression construct (humanized S. pyogenes Cas9 containing N-terminal FLAG-tag and the TET ON promotor) and the pLKO5.sgRNA.EFS.GFP vector were gifts from Eric Lander and David Sabatini and Benjamin Ebert, respectively (Addgene plasmids #50661 and #57822). All sgRNAs in this study were designed using http://crispr.mit.edu/ and quality scores for all but 3 sgRNAs were above 70. Domain description, sgRNA sequences and quality scores from this study are provided in the supplement. sgRNA cloning was performed by annealing and ligating two oligonucleotides into a BsmB1-digested pLKO5.sgRNA.EFS.GFP vector as described[2].

Engineering OCI-AML3-pCW-Cas9: OCI-AML3-pCW-Cas9 cells were derived by retroviral transduction of the *NPM1*^{mut} AML cell line (OCI-AML3) with pCW-Cas9, followed by puromycin selection. Cells were plated in methylcellulose to obtain single cell-derived clones, re-expanded in liquid culture, and aliquots frozen in liquid nitrogen. pCW-Cas9 was induced in each clone with doxycycline and screened by anti-flag western blot analysis for

Cas9 expression. Three independent Cas9 expressing clones were infected with positive control sgRNAs targeting *RPA3* and empty control vector to assess CRISPR-Cas9 editing efficiency after Cas9 induction. The two best performing clones were selected for the *MLL* and *MLL2* domain screen.

sgRNA virus production and negative selection screening: sgRNA virus production was performed in 96-well plates using HEK293T cells using the protocol provided at the Broad's Institute genetic perturbation platform (http://www.broadinstitute.org/rnai/public/resources/protocols) using the envelope and packaging plasmids pCMV-dR8.74psPAX2 and pMD2.G and X-tremeGENE transfection reagent (Roche).

For virus transduction, OCI-AML3-pCW-Cas9 clones were thawed, plated in 96-well plates, and infected using virus supernatant. Three days following infection, GFP+/GFP- ratio was determined and doxycycline was added to the media to induce pCW-Cas9. GFP+/GFP- ratio was tracked every three days for 18 days as described[3].

Analysis, interpretation, and cutoffs: Frequency and spectrum of CRISPR-Cas9 mutagenesis from this assay was investigated in a recent paper by Shi et al[3]. Induction of homozygous frame-shift mutations (44%), and later pairing of heterozygous frame-shift mutations (66% of the remaining population over time) will generally result in a relevant number of null mutations and a drop of GFP positivity over time (for all sgRNAs)[3]. However, sgRNAs that target exons encoding functionally important domains will produce much more null mutations than sgRNAs targeting non-essential domains, since both in-frame and frame-shift mutations will disable the protein. To define dependencies, we set an arbitrary cut-off value to a GFP fold-depletion of 5 for values measured between day 0 and day 15.

SURVEYOR Assays

Genomic DNA (gDNA) was isolated at indicated time points post-infection using QiAamp DNA mini kit (Qiagen #51304) following the manufacturer's instructions. To amplify mutagenized DNA for determination of CRISPR-Cas9 editing efficiency, we amplified 20 ng of gDNA by PCR using a primer set specific for the sgRNA-targeted region with the high-fidelity Platinum Pfx DNA Polymerase (Invitrogen) following the manufacturer's instructions. All primers were optimized to ensure their selectivity for a single genomic region. In addition, due to high GC content of exon 1, PCR was performed using a 2x concentration of the PCR enhancer solution and a nested PCR approach was performed using the following touchdown protocol: 1st PCR with 20ng gDNA template and 25µl reaction volume: 1x 94 5min; 3x 94°C 15s, 61°C 30s, 68°C 60s; 3x 94°C 15s, 58°C 30s, 68°C 60s; 35x 94°C 15s, 55°C 30s, 68°C 60s; 68°C 7min. 2nd PCR with 2µl from PCR reaction 1 in 50µl total reaction volume using the same touchdown PCR conditions with only 30 cycles of the 55°C amplification step and using the same primer sets (primer sequences for both sgRNAs were the same: *MLL1* exon 1 FW: CAGAGCTGGTTAGGCAGGTT and RV: ATTGGGATGCTCCTCAATCC. The PCR products were subjected to SURVEYOR assay (Transgenomic #706020) following the manufacturer's protocol and the results evaluated by agarose gel electrophoresis, stained with ethidium bromide.

Cell Viability and Drug Synergy Assays

Proliferation assays were performed as previously described[4]. Briefly, viable cells were counted by flow cytometry using SYTOX Blue (Invitrogen) or DAPI viability stain. Cells were split and replated with fresh media and drug every 3-4 days. For determination of IC_{50} values EPZ4777, MI-2-2, and MI-503 were diluted 2-fold for a total of 9 concentrations plus vehicle

control with the highest concentrations being 10μM, 12μM, and 10μM respectively. Combinatorial drug treatment of serial dilutions of MI-2-2 or MI-503 with EPZ4777 was performed using constant ratios of 1.2:1 and 1:4 for assessment of drug synergism. Mathematical synergy testing was performed using CompuSyn software for Chou-Talalay-method based calculations[5].

Quantitative real-time PCR

RNA was isolated with the RNeasy mini kit (Qiagen) and then used as a template for cDNA synthesis using the Tetro cDNA kit (Bioline). Quantitative real-time PCR reactions were carried out using SYBR Green or TaqMan MasterMix on an Applied Biosciences qPCR cycler. Relative expression was determined by the Δ/ΔCT method and normalized to the internal control, GAPDH or Actin.

RNA sequencing

Before RNA extraction the same amount of External-RNA-Controls-Consortium (ERCC) synthetic spike-in mix 1 was added to $1x10^6$ freshly lysed cells from each specimen prior to RNA isolation for later normalization. The amount of spike-in added was calibrated to the expected RNA yield of the cells to ensure the spike-in signal was in the appropriate dynamic range (ERCC User Guide, Table 4). RNA was extracted using the RNeasy Mini Kit (Qiagen) including on column DNAse treatment. For gene expression analysis, RNA quality control and quantification was performed using the Agilent Bioanalyzer and the Quant-IT RiboGreen RNA Assay Kit (ThermoFisher). Library construction using poly-A selection was performed using the Illumina TruSeq protocol and sequencing was performed on an Illumina HiSeq 2500 instrument. For gene expression analysis 50 base-pair single read sequencing was performed

using a sequencing depth of 80 Million reads, for the detection of gene fusions 100 base-pair paired-end sequencing at a depth of 80 Million reads.

For gene expression analysis, reads were mapped to the human genome genome (hg19) using TopHat (version 2). Prior to differential gene expression, read counts were either normalized to median read count or to ERCC spike-in controls as described[6]. Differentially expressed genes between DMSO and EPZ4777 treated samples were calculated using DESeq (version 2).

Gene Set Enrichment Analysis (GSEA) was performed as described[7] using the software available at http://software.broadinstitute.org/gsea/index.jsp.

For fusion gene detection sample processing was performed as described above with the exception that no ERCC spike-in controls were added to the samples. Computational prediction of fusion transcripts the Defuse algorithm was used as described.

Results were made publicly available at Gene Expression Omnibus (accession code: GSE85107).

Immunoblotting

Cells were harvested and lysed in SDS–PAGE sample buffer at five million cells per milliliter. Twenty microliters of cell lysate was loaded in each lane. Proteins were resolved by 10% NuPAGE (Invitrogen), transferred to a nitrocellulose membrane (Novex) and probed with the indicated antibodies.

Chromatin Immunoprecipitation

Chromatin immunprecipitation (ChIP) followed by qRT-PCR was performed as previously described[8]. Briefly, cross- linking was performed with 1% formalin for 10min followed by cell

lysis in SDS buffer. Sonication was used to fragment DNA. ChIP for H3K79me2, H3K4me3, Menin, and RNA Polymerase II was performed using the antibodies ab3534 (abcam), 300-150 (Bethyl), ab8580 (abcam) and Santa Cruz sc-899 (Rpb1 N-terminus) specific to the respective modifications. A Normal rabbit IgG 12-370 (Merck Millipore) antibody was used as a control. Eluted DNA fragments were analyzed using qPCR.

Small Molecule Inhibitors

EPZ004777 was synthesized by James Bradner's laboratory (Dana Farber Cancer Institute, Boston, MA). EPZ-5676 and MI-2-2 were purchased from Chempartner. MI-503 was prepared by WuXi PharmaTech. For *in vitro* studies 10mM stock solutions were prepared in DMSO and stored at -20°C. Serial dilutions of stock solutions were carried out just prior to use in each experiment, and final DMSO concentrations were kept at or below 0.01% and 0.02% for combination treatment experiments, respectively. For *in vivo* applications MI-503 was administered intraperitoneally at 50mg/kg in 25% DMSO, 25% PEG 400, and 50% normal saline twice daily.

Primary human AML Co-Culture Assay

Human AML samples were co-cultured with irradiated Hs27 stromal cells for 10 days in serum-free media (StemSpan, Stem Cell Technologies) supplemented with human cytokines, SR-1, and drug(s) or vehicle (DMSO, EPZ004777 10µM, MI-503 2.5µM, or EPZ004777 plus MI-503) as previously described[4]. Drug treatment assays of each individual AML sample were performed only once in three replicates due to limited numbers of viable cells from these specimens. DMSO concentrations were kept below 0.02%. Cell numbers were

determined by flow cytometry using viability and anti-hCD45 staining to control for possible stromal cell contamination after 10 days.

Data Analysis and Statistical Methods

Dose effect curve fitting of drug treatment proliferation assays was performed using the "EC50 shift" non-linear regression model in Graph Pad Prism, version 6 in Figures 2A, 2F, 5C, 6A, and 6B. P-values for differences in gene expression (Fig.2B, 2E, 2I, 5B, 6E, and 6F), ChIP-signal (Fig.3A, 3C, 3D, and 4F), colony count (Fig.2D, 4D, and 6C), apoptosis (Fig. 6H), cell number (Fig.7A), leukemia engraftment (Fig.2H), and white blood cell count (Fig.5E, 7D) were performed using the Student's *t*-test, assuming a two-sample equal variance with normal distribution (in Graph Pad Prism, version 6). No correction for multiple testing was performed. Kaplan-Meier survival estimates were also performed in Graph Pad Prism (version 6) and p-values for survival differences between the groups were calculated using the log-rank (Mantel Cox) test (Fig.2J, 5F, 7C). The whiskers of box plots in Figures 2H, 2I, and 4A represent minimal and maximal values, the box represents the standard error of the mean. The investigators were not blinded to the sample groups for all experiments.

SUPPLEMENTAL REFERENCES

1. Huang J, Gurung B, Wan B, et al. The same pocket in menin binds both MLL and JUND but has opposite effects on transcription. Nature 2012;482:542-6.

2. Heckl D, Kowalczyk MS, Yudovich D, et al. Generation of mouse models of myeloid malignancy with combinatorial genetic lesions using CRISPR-Cas9 genome editing. Nature biotechnology 2014;32:941-6.

3. Shi J, Wang E, Milazzo JP, Wang Z, Kinney JB, Vakoc CR. Discovery of cancer drug targets by CRISPR-Cas9 screening of protein domains. Nature biotechnology 2015;33:661-7.

4. Kühn MWM, Hadler MJ, Daigle SR, et al. MLL partial tandem duplication leukemia cells are sensitive to small molecule DOT1L inhibition. Haematologica 2015;100:e190-3.

5. Chou TC. Theoretical basis, experimental design, and computerized simulation of synergism and antagonism in drug combination studies. Pharmacol Rev 2006;58:621-81.

6. Loven J, Orlando DA, Sigova AA, et al. Revisiting global gene expression analysis. Cell 2012;151:476-82.

7. Subramanian A, Tamayo P, Mootha VK, et al. Gene set enrichment analysis: a knowledge-based approach for interpreting genome-wide expression profiles. Proc Natl Acad Sci U S A 2005;102:15545-50.

8. Chen CW, Koche RP, Sinha AU, et al. DOT1L inhibits SIRT1-mediated epigenetic silencing to maintain leukemic gene expression in MLL-rearranged leukemia. Nat Med 2015;21:335-43.